NeuroImage **13,** 684–701 (2001)
doi:10.1006/nimg.2000.0715, available online at http://www.idealibrary.com on IDEAL®

Human Primary Auditory Cortex: Cytoarchitectonic Subdivisions and Mapping into a Spatial Reference System

P. Morosan,* J. Rademacher,† A. Schleicher,‡ K. Amunts,* T. Schormann,§ and K. Zilles*,‡,§,[1]

Institute of Medicine, Research Center Jülich, Jülich; and ‡C&O Vogt Institute for Brain Research, §Department of Neuroanatomy, and †Department of Neurology, Heinrich-Heine University, 40225 Düsseldorf, Germany

Received June 30, 2000; published online February 2, 2001

The transverse temporal gyrus of Heschl contains the human auditory cortex. Several schematic maps of the cytoarchitectonic correlate of this functional entity are available, but they present partly conflicting data (number and position of borders of the primary auditory areas) and they do not enable reliable comparisons with functional imaging data in a common spatial reference system. In order to provide a 3-D data set of the precise position and extent of the human primary auditory cortex, its putative subdivisions, and its topographical intersubject variability, we performed a quantitative cytoarchitectonic analysis of 10 brains using a recently established technique for observer-independent definition of areal borders. Three areas, Te1.1, Te1.0, and Te1.2, with a well-developed layer IV, which represent the primary auditory cortex (Brodmann area 41), can be identified along the mediolateral axis of the Heschl gyrus. The cell density was significantly higher in Te1.1 compared to Te1.2 in the left but not in the right hemisphere. The cytoarchitectonically defined areal borders of the primary auditory cortex do not consistently match macroanatomic landmarks like gyral and sulcal borders. The three primary auditory areas of each postmortem brain were mapped to a spatial reference system which is based on a brain registered by *in vivo* magnetic resonance imaging. The integration of a sample of postmortem brains in a spatial reference system allows one to estimate the spatial variability of each cytoarchitectonically defined region with respect to this reference system. In future, the transfer of *in vivo* structural and functional data into the same spatial reference system will enable accurate comparisons of cytoarchitectonic maps of the primary auditory cortex with activation centers as established with functional imaging procedures.

[1] To whom correspondence and reprint requests should be addressed at the C&O Vogt Institute for Brain Research, Heinrich-Heine University, Universitätsstrasse 1, 40225 Düsseldorf, Germany. Fax: +49-211-8112336. E-mail: zilles@hirn.uni-duesseldorf.de.

Key Words: **human cerebral cortex; auditory cortex; cytoarchitecture; image analysis; brain mapping.**

INTRODUCTION

The cytoarchitectonically defined area 41 of Brodmann (1909) represents the putative anatomical correlate of the human primary auditory cortex (PAC). It is located in the depth of the Sylvian fissure where it occupies most of Heschl's gyrus (HG). According to Brodmann (1909), area 41 is surrounded caudolaterally by area 42, rostrolaterally by area 22, and medially by area 52 (Fig. 1) on the superior temporal plane.

Although HG is usually defined as the site of PAC, existing cytoarchitectonic parcellation schemes of PAC vary among different available maps. While Brodmann (1909) described only one koniocortical area (area 41) as PAC, others have identified two areas within the primary auditory cortex (Economo and Koskinas, 1925; Sarkissov *et al.,* 1955; Galaburda and Sanides, 1980). Moreover, the size and exact location of areal borders and anterior-to-posterior or medial-to-lateral distribution of these areas differ between the studies, and the intersubject variability of cytoarchitecture, size, and topography was not analyzed (Lashley and Clark, 1946). It is not known to what degree divergent anatomical patterns may reflect interindividual variability or only interobserver differences caused by the highly observer-dependent methods of classical architectonic studies. The classical maps do not include data on variations in topography or size of PAC between the hemispheres and/or the sexes. Finally, the 2-D presentation in highly schematized maps of the previous cytoarchitectonic parcellations are of limited use for comparisons with functional imaging studies based on 3-D data sets from living human brains.

Noninvasive *in vivo* analysis of auditory perception has been accomplished with electroencephalography (Celesia, 1976; Liegeois-Chauvel *et al.,* 1991, 1994), magnetoencephalography (Reite *et al.,* 1982; Romani *et al.,* 1982a; Hari *et al.,* 1984; Pantev *et al.,* 1989a; Hari,

1053-8119/01 $35.00

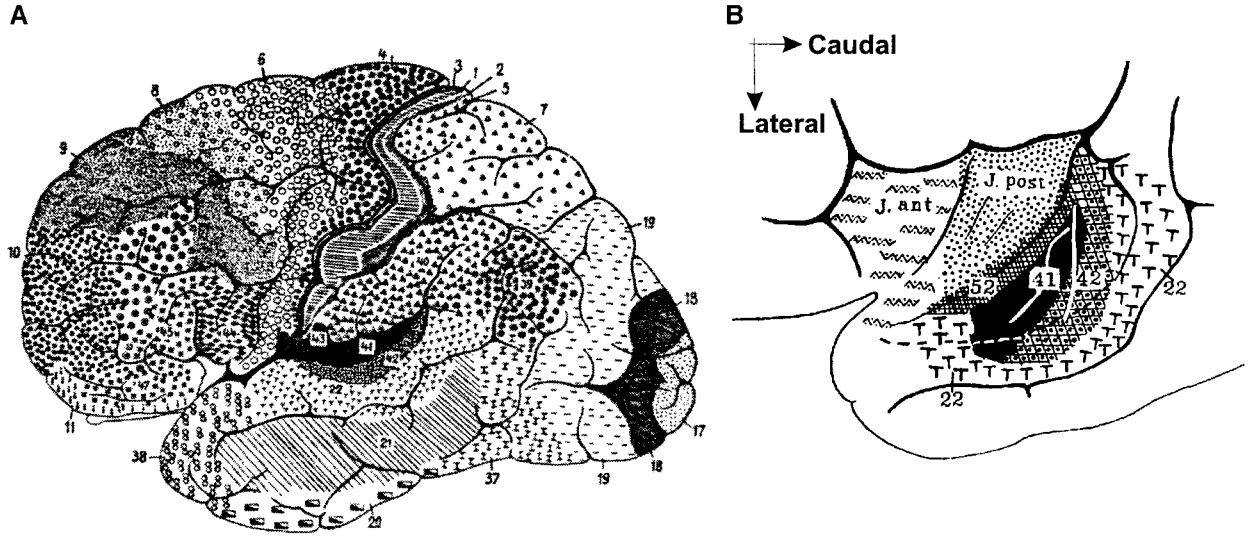

FIG. 1. Topography of the primary auditory cortex (area 41, solid black) in the cytoarchitectonic map of Brodmann (1909). (A) Lateral view. (B) View of the supratemporal plane in the depth of the Sylvian fissure.

1991; Scheuneman *et al.*, 1991; Yoshiura *et al.*, 1995; Langner *et al.*, 1997), and functional imaging, including magnetic resonance imaging (Binder *et al.*, 1994; Strainer *et al.*, 1997; Scheich *et al.*, 1998; Schmid *et al.*, 1998; Talavage *et al.*, 1999). Most of these studies have demonstrated that primary auditory functions such as the response to pure tones and to acoustic frequency patterns map onto the medial two-thirds of HG. Several studies provided evidence for a tonotopic organization of the functionally defined primary auditory cortex (A1) with responses to low-frequency stimuli originating more laterally and high-frequency stimuli originating more medially (Romani *et al.*, 1982b; Hari *et al.*, 1984; Lauter *et al.*, 1985; Pantev *et al.*, 1989b, 1995; Yamamoto *et al.*, 1992; Tiitinen *et al.*, 1993; Reite *et al.*, 1994; Verkindt *et al.*, 1995; Howard *et al.*, 1996; Talavage *et al.*, 1997; Ottaviani *et al.*, 1997; Bilecen *et al.*, 1998).

In contrast to the established functional lateralization of language, asymmetries following acoustic stimulation are still a matter of discussion (Matsumiya *et al.*, 1972; Reite *et al.*, 1981; Lauter, 1992; McFadden, 1993; Polyakov and Pratt, 1995; Poeppel *et al.*, 1996; Belin *et al.*, 1998; Zouridakis *et al.*, 1998; Nicholls, 1998; Pantev *et al.*, 1998a).

Since a considerable intersubject variability in size, shape, and topography of the transverse gyri has been described (Steinmetz *et al.*, 1989; Thompson *et al.*, 1996; Penhune *et al.*, 1996; Leonard *et al.*, 1998), this variability of macroscopical landmarks should be taken into account in an architectonic analysis and when interpreting putative structural–functional correlations. It is not known whether the functionally defined PAC maps precisely onto the cytoarchitectonically defined PAC, although studies of other cortical regions indicate that microstructurally defined (i.e., cytoarchitecture) cortical areas may precisely parallel functionally defined areas (Merzenich *et al.*, 1978; Kaas *et al.*, 1979; Iwamura *et al.*, 1994; Roland and Zilles, 1998). However, a reliable and sufficiently precise localization of the borders of cytoarchitectonic areas on the basis of gyral or sulcal landmarks is problematic as previously demonstrated (Rademacher *et al.*, 1993; Rajkowska and Goldman-Rakic, 1995; Amunts *et al.*, 1999). Thus, a mapping of cytoarchitectonic and functional images to a common reference space is required for further testing the hypothesis of architectonic/functional parallels and the value of macroscopical landmarks for this question.

We used a recently described observer-independent cytoarchitectonic method (Schleicher *et al.*, 1999) for the reliable definition of PAC and its areal borders. In contrast to classical architectonic studies based on pure visual inspection and individual pattern recognition capabilities, this method uses quantitative data and multivariate statistics to provide reproducibility, reliability, and precision of the results. The measurements were performed with an automated microscopic scanning and image analysis procedure, which enables the detection of the sites of statistically significant changes in laminar distribution of volume densities of cell bodies, the most important cytoarchitectonic criterion (Zilles *et al.*, 1995; Geyer *et al.*, 1996, 1999; Amunts *et al.*, 1999). The cytoarchitectonically defined areas and their borders were reconstructed three-dimensionally and visualized in the stereotaxic space of a reference brain (Roland and Zilles 1994, 1996, 1998). This approach also provides a tool to calculate probability maps of PAC by superimposing the PACs of different postmortem brains onto the format of the stan-

TABLE 1

Brains Selected for the Present Study

Case	Brain code	Age (years)	Gender	Cause of death	Postmortem delay (h)	Brain weight (g)[a]	Fixation
1	16/96	54	Male	Cardial infarction	8	1757	Formalin
2	146/86	37	Male	Cardiac arrest	24	1437	Formalin
3	544/91	79	Female	Carcinoma of the bladder	24	1350	Bodian
4	207/84	75	Male	Acute glomerulonephritis	24	1349	Formalin
5	2/95	85	Female	Mesenteric infarction	14	1046	Bodian
6	281/93	68	Male	Cardiovascular disease	16	1360	Formalin
7	382/81	59	Female	Cardiorespiratory insufficiency	24	1142	Formalin
8	68/95	79	Female	Cardiorespiratory insufficiency	16	1110	Bodian
9	24/31	39	Male	Drowning	10	1247	Formalin
10	56/94	72	Female	Renal failure	12	1216	Formalin

[a] Prior to fixation.

dard brain (Mazziotta *et al.*, 1995) (see companion article by J. Rademacher *et al.*).

The goals of our study are the: (i) quantitative cytoarchitectonic definition of PAC and its subdivisions, (ii) analysis of side and gender differences in cytoarchitecture, and (iii) mapping of PAC and its subdivisions to the *in vivo* format of the standard reference brain.

MATERIALS AND METHODS

Subjects

Ten adult human postmortem brains were obtained from the body donor program of the Anatomical Institute of the University of Düsseldorf in accordance with legal requirements (Table 1). None of the subjects had clinical records of previous neurological or psychiatric disorders. Handedness of the subjects was unknown.

MR Imaging and Histological Processing of Postmortem Brains

The complete undissected brains were fixed in 4% formalin or in Bodian's solution (mixture of formalin, glacial acetic acid, and ethanol). The postmortem delay was between 8 and 24 h. MR imaging of each postmortem brain was performed with a Siemens 1.5-T scanner (Erlangen, Germany) with a T1-weighted FLASH sequence covering the entire brain (flip angle 40°, repetition time TR = 40 ms, echo time TE = 5 ms for each image) for the documentation of brain morphology and dimensions before histological processing (Roland and Zilles, 1994). Spatial resolution was $1 \times 1 \times 1.17$ mm. After MR imaging, all brains were dehydrated in a graded series of alcohol, embedded in paraffin, and serially sectioned in the coronal plane (20-μm-thick sections). Every 15th section was silver stained for demonstrating cell bodies, i.e., cytoarchitecture (Merker, 1983). Every 60th section was used for quantitative cytoarchitectonic analysis and 3-D reconstructions of the brains (see below).

Measurements of Cell Volume Densities (GLI)

Cortical regions large enough to include PAC and neighboring areas were interactively marked as regions of interest (ROI). Within each ROI, quantification of cell volume densities was performed using the gray level index (GLI) procedure (Schleicher and Zilles, 1990; Schleicher *et al.*, 1999). In brief, each ROI was completely covered by a continuous, mosaic-like pattern and scanned using TV frames 524×524 μm in size, 512×512-pixel spatial resolution, and 8-bit gray resolution at low microscopical resolution (Planapo 4.0×1.25; Zeiss, Germany). From each TV frame, a binary image is generated by adaptive thresholding (Castleman, 1979) which is further subdivided by a grid of $k \times k$ measuring fields. The size of each measuring field defines the spatial resolution of the scanning procedure. In the present paper, the GLI ($0\% \leq \text{GLI} \leq 100\%$) is the areal fraction of cellular profiles in a measuring field of 32×32 μm. The GLI is correlated with the volume density of neurons (Wree *et al.*, 1982). Because the GLI is a *ratio* of the areal projections of two volumes (cell bodies and neuropil), it is not distorted by histological processing as both compartments are expected to shrink to the same degree (Amunts *et al.*, 1999).

Observer-Independent Localization of Areal Borders

The quantitative cytoarchitectonic procedure for determining areal borders was already published in detail (Schleicher *et al.*, 1999). Therefore, only a brief description of the principles will follow here. Changes of the GLI extending from layer II to the gray/white matter boundary were registered vertically to the cortical surface along traverses through the cortex with

equidistant intervals (128 μm) between each other. Each traverse indicates an individual GLI profile (ordinate, cell volume density (%); abscissa, total cortical thickness normalized to 100%).

For a quantitative analysis of the cytoarchitecture represented by the shape of GLI profiles, each individual profile was characterized by a set of 10 features (feature vector), comprising the mean GLI value (mean*y*.o = mean cell volume density averaged over all cortical layers), the center of gravity in *x* direction (mean*x*.o), the standard deviation (SD.o), the skewness (skew.o), the kurtosis (kurt.o) of each profile curve, and the analogous parameters for the first derivative (mean*y*.d, mean*x*.d, SD.d, skew.d, kurt.d). These features were calculated as central moments by treating the profile and its differential quotient as frequency polygons. The data from all profiles of a ROI were standardized to *Z* scores in order to assign equal weight to each of the features.

The Mahalanobis distances (D^2) between the feature vectors of the profiles located in two neighboring cortical sectors were calculated. The width of a sector was varied systematically so that each sector comprised between 8 (1024 μm) and 24 profiles (3072 μm). D^2 quantifies the degree of dissimilarity in laminar pattern (difference in cytoarchitecture) between two neighboring sectors. D^2 was calculated for all sequential positions of the two neighboring cortical sectors, if both sectors were shifted simultaneously like sliding windows by 128 μm to the next position, i.e., the distance between two individual profiles. This procedure results in several sets of Mahalanobis distances for the systematically varied widths (see above) of the cortical sectors (Schleicher *et al.*, 1999) and, thus, in calculations of D^2 at varying levels of spatial resolution. Positions of profiles were indexed from 1 (starting position) to *n* (final position), where *n* was the total number of profiles per ROI. D^2 values were plotted along the positions 1 to *n* resulting in a Mahalanobis distance function. Maxima of this function D^2 indicate large differences in cytoarchitecture between two neighboring sectors. In contrast to the Euclidean approach, the Mahalanobis approach to localize cytoarchitectonic areal borders has a pronounced sensitivity to abrupt changes in the laminar pattern, which are expected at the border between two cortical areas. It is less sensitive to gradual changes in cytoarchitecture caused by cortical folding (Schleicher *et al.*, 1999). Since only ROIs showing a clear six-layered cortex were used for the observer-independent localization of areal borders, only gradual changes in cytoarchitecture were induced by cortical folding. Thus there is no indication that the Mahalanobis approach is affected by cortical folding in this application. The Mahalanobis distance can be tested using the Hotelling T^2 test for proving the significance of a difference between the mean vectors of two multivariate distributions. We applied this test in combination with a Bonferroni adjustment of the *P* values for multiple comparisons (Dixon *et al.*, 1988). Significant maxima define putative cytoarchitectonic areal borders, which were selected according to the following definitions: (i) discard maxima with $P > 0.05$ in the Hotelling T^2 test (statistical criterion); (ii) accept only the absolutely highest maximum as a putative areal border, if two or more, significant (P value $<$ 0.05) maxima are spatially separated by less than the actual size of one sector (resolution criterion); and (iii) consider only those maxima as areal borders which were found at comparable positions across a series of at least three adjoining histological sections (consistency criterion).

Quantitative Cytoarchitecture of Cortical Areas

In each brain and each cytoarchitectonically identified area, 10 to 15 individual GLI profiles were randomly selected and averaged to generate a mean GLI profile curve, which represents the areal- and brain-specific cytoarchitectonic organization. For areas Te1.2, Te1.0, and Te1.1 a total number of 60 mean GLI profiles resulted (3 mean GLI profiles for the three areas × 2 hemispheres × 10 brains).

By projecting the mean GLI profile curve of an area onto the corresponding histological image via a drawing tube attached to a microscope, the borders between cortical layers were identified by visual inspection. This procedure enables the measurement of relative (total cortical thickness was normalized to 100%, see above) thickness and cell volume density (GLI) of each cortical layer. Interareal, side, and gender differences in total and lamina-specific GLI and in relative thickness of each layer were tested by analysis of variance (ANOVA) using a repeated-measures design. Significant differences were further analyzed by paired *t* tests (Bonferroni corrected for multiple comparisons).

Cytoarchitectonic Variability of Cortical Areas

Intersubject Variability of Cytoarchitecture of a Distinct Cortical Area

Between-subject dissimilarity of the laminar pattern of the same cytoarchitectonic area was measured by calculating Euclidean distances between two sets of profiles of the same area sampled from all possible pairs of different brains in the total sample of 10 brains; i.e., feature vectors of individual GLI profiles of corresponding areas between all different brains were compared. In contrast to the border-locating procedure using the Mahalanobis distance, we calculated Euclidean distances as a measure of dissimilarity, since the Euclidean distance is the distance between two centroids of *p*-dimensional clusters and is not affected by the degree of variability within clusters. Mahalanobis distances, however, are calculated using an internal

standardization of the data, which is specific for each pair of sets of profiles. In our sample of 10 brains, 45 distance values between all unique pairs of brains were calculated for each area. The average of these 45 values was defined as the "intersubject distance" of an area. High intersubject distances indicated a high degree of dissimilarity between the same set of cortical areas in different brains, i.e., high degree of intersubject cytoarchitectonic variability.

Interareal Variations of Cytoarchitecture in a Subject

To address the question whether intersubject cytoarchitectonic variability can obscure differences between areas in individual brains, we measured interareal dissimilarities of the area-specific laminar patterns between two different areas of the same brain. We calculated Euclidean distances for all possible unique pairs of areas Te1.1, Te1.0, and Te1.2 and one neighboring, non-primary auditory area (Brodmann area 52, TI1 in the present study). This approach produces six different comparisons of areas and thus six distance values in each brain. Corresponding interareal distances were averaged over the sample of 10 brains (interareal distances). Interareal distances were compared with a "reference distance," i.e., the grand average distance calculated from all the intersubject distances of the cortical areas included in the actual comparison. Interareal distances which are lower than the reference distance indicate that interareal variations of the laminar pattern can be obscured by intersubject differences between corresponding cortical areas. Higher interareal than intersubject differences indicate that the cytoarchitectonic pattern of a given area is robust across individuals and not obscured by intersubject variability in cytoarchitecture.

Mapping to a Spatial Reference System

Position and extent of areas Te1.2, Te1.0, and Te1.1 in the histological sections were mapped to a spatial reference system, which is represented by an *in vivo* acquired 3-D MR data set of an individual brain with no history of neurological or psychiatric diseases (Roland and Zilles, 1994; Geyer *et al.*, 1999; Amunts *et al.*, 1999, 2000). For this purpose, the histological sections were digitized and 3-D reconstructed (histological volume). Mapping of the histological volumes to the corresponding MR volumes, which were obtained prior to embedding and sectioning, allowed the correction of deformations inevitably resulting from the histological procedure. This matching was performed by using both linear and nonlinear transformations (Schormann *et al.*, 1993, 1995, 1996). Finally, the postmortem brains were warped to the MR volume of the standard spatial reference system using affine transformations (Schormann and Zilles, 1997, 1998). The affine transformations normalized absolute brain sizes (scaling) and included also rotation and translation without changing individual brain anatomy. The spatially normalized brains were orientated in the AC–AP plane (Talairach and Tournoux, 1988). The positions and extents of the cytoarchitectonically defined primary auditory areas were traced interactively onto the digitized histological sections using an image analyzer system (KS400). The labeled cytoarchitectonic areas were 3-D reconstructed and spatially normalized using the same transformations as were applied for the whole brains. In a final step, the spatially normalized areas were also oriented in the AC–AP plane (Talairach and Tournoux, 1988).

We studied the relationship between macroanatomical landmarks and cytoarchitectonically defined areal borders in each affine-transformed brain by comparing the Talairach coordinates of the framing sulci of the Heschl gyrus with the coordinates of the cytoarchitectonically defined borders of the whole primary auditory cortex (Te1).

RESULTS

Descriptive Cytoarchitecture

Region Te1 (Brodmann area 41) is located on the Heschl gyrus and is microscopically identifiable as a highly granular cortex (koniocortex), which is surrounded by less granular cortices, areas Te2, Te3, and TI1. Te1 is characterized by the occurrence of small granular cells throughout the entire cortical depth, small-sized pyramidal cells of layer IIIc, a prominent layer IV, and a relatively cell-sparse layer V. Medially, Te1 is bordered by the insular cortex and anterolaterally by area Te3 (part of Brodmann area 22). In comparison to Te1, area Te3 is characterized by a less granular appearance, the occurrence of larger pyramidal cells in layer IIIc, smaller width of layer IV, and a higher cell density in layer V. Rostrally, Te1 is bordered by the temporoinsular area TI1 (Brodmann parainsular area 52). The latter is characterized by a wider supragranular (especially layer III) compared to infragranular layers, narrow layer IV, and high cell densities in layers V and VI. Caudolaterally, Te1 is bordered by area Te2 (Brodmann area 42), which is less granular than Te1 and contains large pyramidal cells in layer IIIc.

Areal Borders of Te1

Outer Borders of the Whole Primary Auditory Cortex Te1

The areal borders of Te1 with the surrounding areas TI1, Te2, and Te3 were defined in each individual brain. Figure 2 shows an example of the observer-independent definition of areal borders between Te2, Te1, and TI1. A digitized high-resolution histological

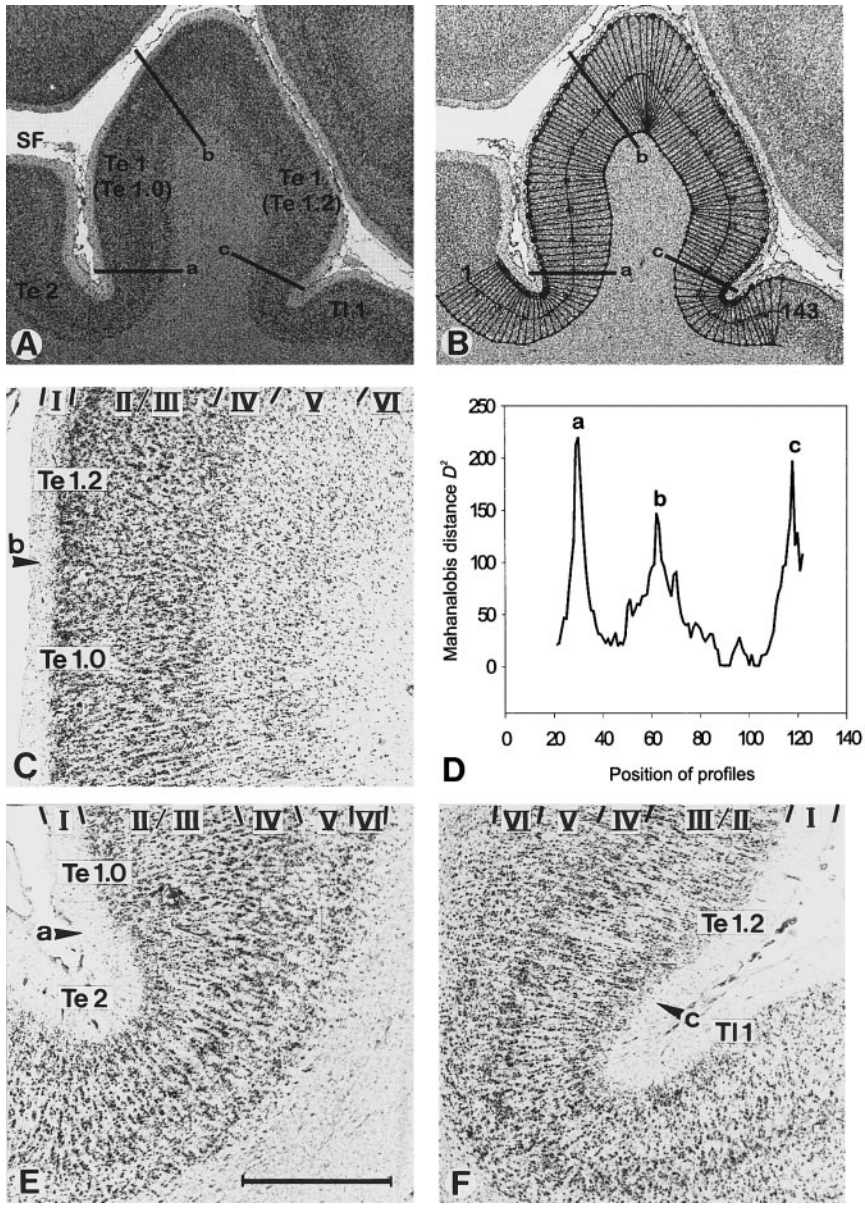

FIG. 2. Example of the observer-independent cytoarchitectonic definition of areal borders. (A) Digitized histological and cell-body stained section with areas Te2, Te1 (Te1.2 and Te1.0), and TI1. SF, Sylvian fissure. (B) GLI image of A. A high GLI is represented by a dark pixel, a lower GLI is visualized by a lighter pixel. The cortex was sampled with equidistant traverses from layer II to the gray/white matter boundary. The positions of the profiles were numbered from 1 to 143. (C) Photomicrograph showing the border between areas Te1.0 and Te1.2; arrowhead "b" corresponds to GLI profile 53 in B and maximum "b" in D. (D) The Mahalanobis distance D^2 was plotted against the position of GLI profiles (distance function). The significant maxima of the distance function D^2 at positions "a", "b," and "c" exactly match the borders between Te1.0/Te 2 (B), Te1.0/Te2 (E), and Te1.2/TI1 (F), respectively. (E) Photomicrograph of the border between areas Te1.0 and Te2; arrowhead "a" corresponds to GLI profile 30 in B and maximum "a" in D. (F) Photomicrograph of the border between areas Te1.2 and TI1; arrowhead "c" corresponds to GLI profile 120 in B and maximum "c" in D. Roman numerals in C, E, and F indicate cortical layers. Scale bar, 1 mm.

image (Fig. 2A) was converted into the corresponding GLI image ("protocol image," Fig. 2B), in which 143 individual GLI profiles were traced equidistantly. This protocol image contains positions a, b, and c of significant maxima of the Mahalanobis distance function D^2 shown in Fig. 2D. Comparisons of these maxima with the original histological images are provided in Figs. 2E and 2F. Figure 2E shows the cytoarchitectonic changes at the border between area Te2 and Te1 (Te1.0, see below), corresponding to maximum a. Figure 2F shows the cytoarchitectonic changes at the border between Te1 (Te1.2, see below) and TI1, corresponding to maximum c. The border between Te1 and Te3 is shown in Fig. 3.

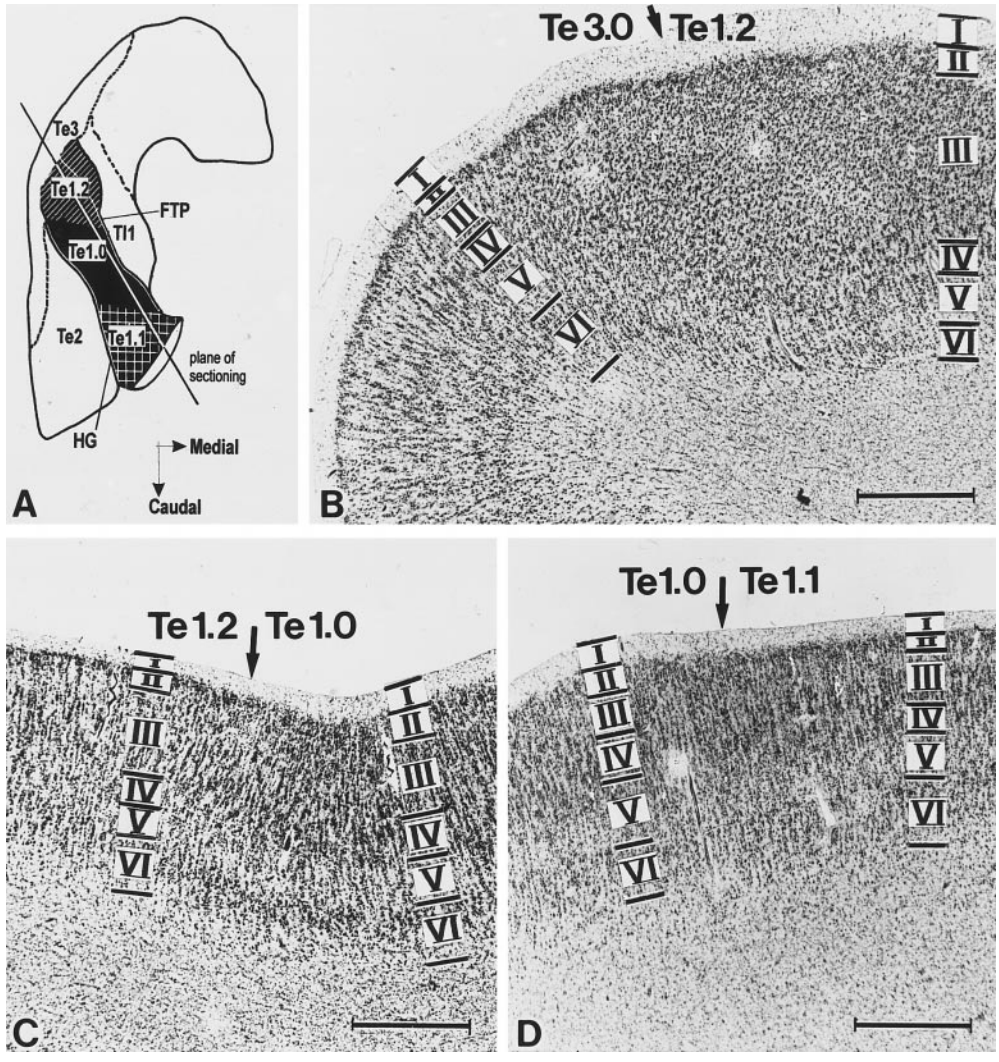

FIG. 3. (A) Topography of areas Te1.2, Te1.0, and Te1.1 on the superior temporal plane. (B, C, D) Photomicrographs of the Heschl gyrus of one individual brain cut in the sagittal plane (not included in our present quantitative cytoarchitectonic study); arrows indicate the borders between Te3/Te1.2, Te1.2/Te1.0, and Te1.0/Te1.1.

Subdivision of Te1

This method detected also cytoarchitectonic changes within Te1, indicating subdivisions of the primary auditory cortex Te1 into three areas (as an example see Figs. 2A and 2B with line b and Fig. 2C with an arrowhead indicating the position of maximum b). Maximum b subdivides Te1 into areas Te1.0 and Te1.2. The border between Te1.0 and Te1.1 is shown in Fig. 3. In each hemisphere, Te1 could be consistently subdivided into three areas, Te1.1, Te1.0, and Te1.2, following each other in the medial-to-lateral direction (Fig. 3A).

After the observer-independent definition of areal borders we looked for characteristic cytoarchitectonic features of the three areas (Figs. 3 and 4). The centrally located area Te1.0 is characterized by the highest degree of granularization, if compared to its neighboring areas Te1.2 and Te1.1, i.e., the thickest layer IV and particularly small-sized IIIc pyramidal cells. In strictly orthogonally oriented sections, the arrangement of neuronal perikarya in vertical cell columns is found most clearly in area Te1.0 (rain-shower formation of von Economo and Koskinas, 1925). The medially situated area Te1.1 can be characterized by a less distinct cortical layering and the appearance of single, medium-sized pyramidal cells in layer IIIc. Laterally, the granular area Te1.2 shows a broad layer III, which contains clusters of medium-sized IIIc pyramids. This feature can be also seen in the neighboring nonprimary auditory areas.

Quantitative Cytoarchitecture

Figure 4 shows the cytoarchitecture of areas Te1.2, Te1.0, and Te1.1 of three individual subjects (cases 3,

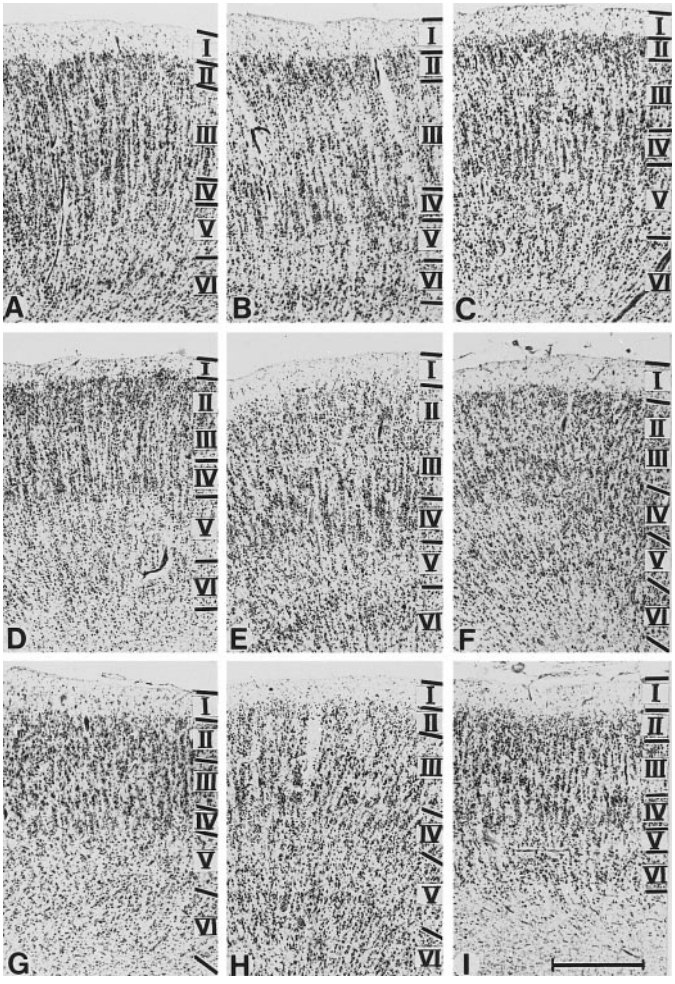

FIG. 4. Photomicrographs of areas Te1.2 (A, B, C), Te1.0 (D, E, F), and Te1.1 (G, H, I) in three individual brains. Roman numerals indicate cortical layers. Scale bar, 1 mm.

4, and 7). The differences in cytoarchitecture between the three primary auditory areas can be recognized in each brain (interareal variability). Between subjects, variations of the laminar patterns of corresponding areas were observed as well (intersubject variability).

To study the interareal and intersubject cytoarchitectonic differences, laminar cell volume densities of each primary auditory area were represented by a corresponding mean GLI profile curve. Figure 5 shows the mean GLI profiles of area Te1.0 in 10 left hemispheres and of areas Te1.2 and Te1.1 in a single left hemisphere. A comparison of the mean GLI profiles (solid lines) of Te1.0 reveals the interindividual variability in cytoarchitecture of an identical area (Fig. 5). The dashed lines (standard error of the mean) demonstrate the intraindividual variability of GLI profiles in Te1.0 (for all cases) and in Te1.1 and Te1.2 (selected representative cases). Each primary auditory area has a high cell density in layers II, lower III, IV, and, to a varying degree, also in VI (represented by consistent maxima of the mean GLI profile curves) and a low cell density in upper layer III and layer V (represented by consistent minima of the GLI profile curves). Interareal and intersubject differences are reflected by differences in shape and the occurrence of inconsistent maxima and minima in the mean GLI profile curves.

Mean areal and laminar cell volume densities and layer thickness were extracted from corresponding mean GLI profile curves of each area (Tables 2 and 3) and tested for interareal, side, and gender differences (ANOVA, repeated-measure design). While there are no gender differences in our sample, significant interactions between the within-factors area and the side are found. Mean areal cell volume densities show significant higher values in Te1.1 compared to Te1.2 in the left, but not in the right, hemisphere, caused by significant differences in layers IV, V, and VI (paired *t* test, $df = 9$, $P < 0.05$). Higher cell volume densities are found on the left side in areas Te1.0 and Te1.1 and on the right side in area Te1.2, but these differences were not significant (paired *t* test, $df = 9$, $P > 0.05$) (Fig. 6). Laminar thickness in the left hemisphere shows significant interareal differences in layer III (paired *t* test, $df = 6$, $P < 0.05$), with higher values in area Te1.2 than in areas Te1.0 and Te1.1 (Fig. 7A). No significant differences can be detected in the right hemisphere. In layer IV of both hemispheres, significantly higher thickness are found in area Te1.0 than in areas Te1.2 and Te1.1 (paired *t* test, $df = 6$, $P < 0.05$) (Fig. 7B).

Cytoarchitectonic Variability of Cortical Areas

The *intersubject* variability of the GLI profiles of each of the auditory areas (Fig. 8A) is highest in area Te1.0 of the left hemisphere (Euclidean distance 2.59) and lowest in area Te1.2 of the left hemisphere (Euclidean distance 1.68). Left–right comparisons of the intersubject differences in cytoarchitecture show a larger variability in area Te1.0 than in areas Te1.2 and Te1.1. This indicates that the left area Te1.0 varies to a higher degree between subjects than the right area Te1.0. The average Euclidean distance calculated from the intersubject distances of all three primary auditory areas is 2.06 on the left side and 1.84 on the right side ("grand average distance" = mean of all comparisons, black line in Fig. 8A).

Interareal differences in cytoarchitecture between four areas (six comparisons of two of four areas) of each hemisphere in the sample of 10 brains are shown Fig. 8B. Since this type of analysis is based on distances between pairs of areas, no absolute positions of the areas in the *p*-dimensional feature space nor any visualization for their mutual arrangement can be derived from the data. However, multidimensional scaling (Henery *et al.*, 1998) is an adequate tool to visualize the mutual arrangement of the areas with correct distances between each possible pair in two dimensions. It

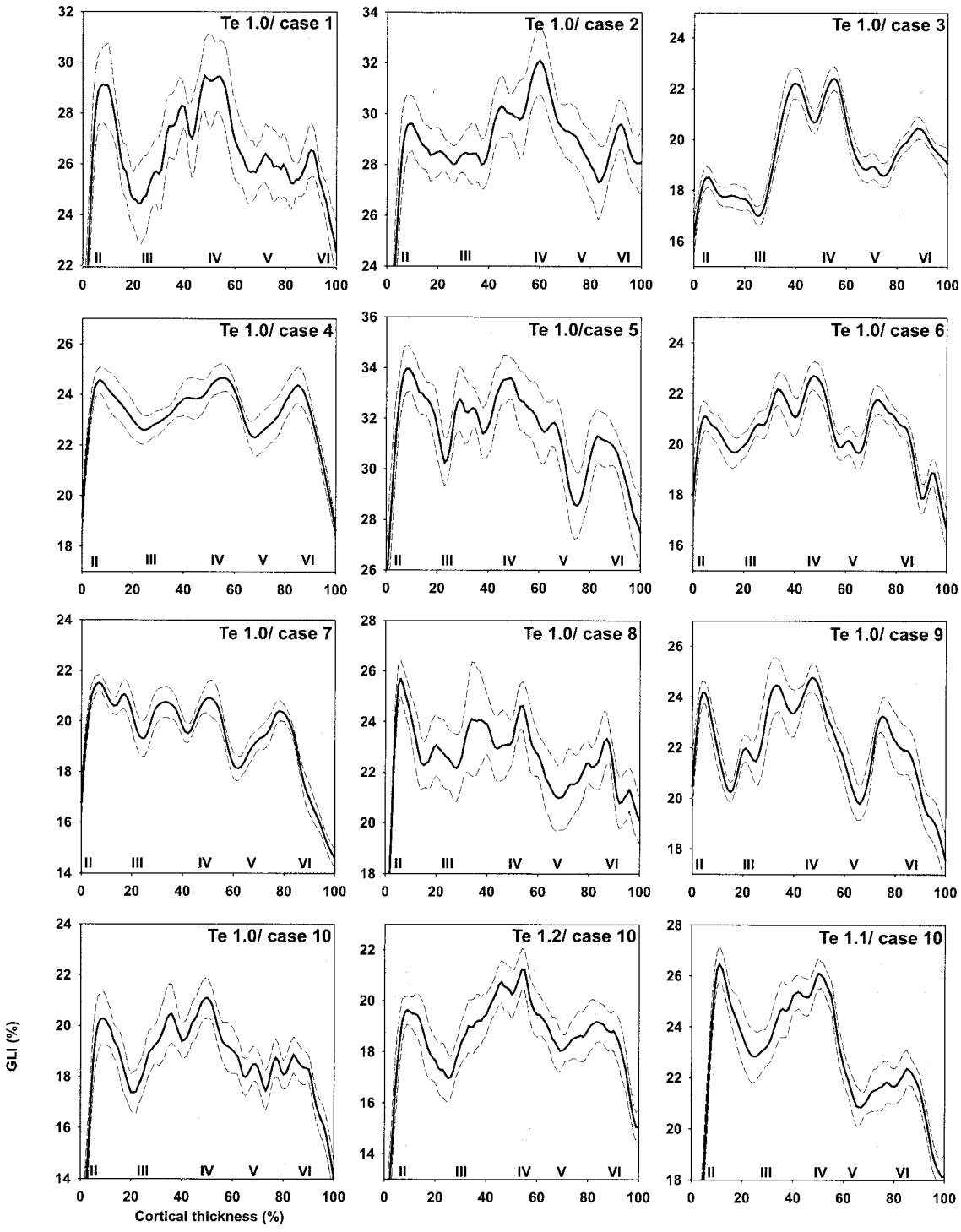

FIG. 5. Mean GLI profile curves of area Te1.0 in 10 left hemispheres and areas Te1.2 and Te1.1 in 1 left hemisphere. Bold lines indicate means, dashed lines indicate standard errors of the means. Areal and brain codes are labeled by Arabic numerals, cortical layers by Roman numerals. Ordinate, GLI (%); abscissa, laminar depth (%).

permits the visualization of areas from a set of observed distances between all pairs by computing coordinates of the areas in two dimensions (dimension 1 and dimension 2 in Fig. 8B) such that the estimated distances between pairs of areas fit as closely as possible to the observed distances in *p* dimensions. Figure 8B demonstrates the interareal distances after multidimensional scaling, which allows a clear and comprehensive presentation of the mutual degree of cytoarchitectonic dissimilarity between the four areas Te1.0,

TABLE 2

Relative Laminar Thickness of Cortical Layers ± SD (%)

	Left			Right		
Layer	Te 1.2	Te 1.0	Te 1.1	Te 1.2	Te 1.0	Te 1.1
II	8.8 ± 3.2	7.4 ± 1.4	9.1 ± 3.3	8.0 ± 2.3	9.8 ± 3.9	8.9 ± 1.3
III	36.7 ± 5.8	35.0 ± 4.3	34.8 ± 4.1	33.6 ± 4.0	26.5 ± 4.4	33.4 ± 5.4
IV	12.3 ± 1.5	16.0 ± 1.6	11.9 ± 1.7	12.7 ± 1.1	15.8 ± 1.2	12.2 ± 1.6
V	21.7 ± 3.8	19.0 ± 4.5	21.2 ± 3.6	23.6 ± 3.9	24.8 ± 3.6	20.8 ± 3.4
VI	20.5 ± 7.0	22.7 ± 5.9	23.0 ± 6.1	22.1 ± 3.3	23.1 ± 5.2	24.7 ± 4.5

Note. The relative thickness of each layer was calculated after normalization of the distance between the layer II/III border and the cortex/white matter border. Because of left–right differences, means of measurements in the left and right hemispheres are presented separately.

Te1.1, Te1.2, and TI1. In both hemispheres, interareal distances between primary auditory areas (Te1.0, Te1.1, and Te1.2) on the one hand and the nonprimary auditory area (TI1) on the other hand are larger than interareal distances between the different primary auditory areas.

To demonstrate the Euclidean distances in cytoarchitecture between each possible interareal comparison in both hemispheres, the interareal differences in cytoarchitecture between the three primary auditory areas averaged over the sample of 10 brains are lower than the intersubject reference distance (grand average of all possible comparisons between primary and nonprimary auditory areas) (Fig. 8C). Thus, interareal differences between primary auditory areas can be obscured by intersubject variations of their laminar pattern. In contrast, the distances between the primary areas on one side and the nonprimary auditory area TI1 on the other side are higher. These findings indicate that the cytoarchitecture of the three primary auditory areas is more similar and, thus, comprises a nearly related set of cytoarchitectonic areas ("cytoarchitectonic family"), i.e., the primary auditory cortex Te1.

Macroanatomical Topography and Spatial Reference System

In all hemispheres, Te1 can be located on HG. In the depth of the Sylvian fissure, the medial origin of HG is separated from the insular cortex by the circular sulcus, while the lateral border of HG cannot be defined by macroanatomical landmarks. HG always separates the supratemporal plane into a rostral and a caudal part, the planum polare and the planum temporale, respectively (for an example, see Fig. 9). The anterior border of HG is consistently marked by the first transverse temporal sulcus. The posterior border of HG is frequently obscured by anatomical variations. Two frequent patterns ("duplications") have been described in the literature (Pfeifer, 1920; Penhune *et al.*, 1996): either the crown of HG is incompletely intended by the intermediate sulcus or there is a complete duplication resulting in two transverse gyri which are separated by the second transverse temporal sulcus (Heschl's sulcus). In our sample of 10 brains, incomplete duplications of HG are found in 5 of 20 hemispheres and complete duplications in 6 of 20 hemispheres. Thus, the localization of Te1 based on macroanatomical landmarks is seriously impaired by these gyral variations and the difficulties in identification. Especially the medial-to-lateral extent of Te1 and its areas cannot be precisely defined by gyral features or other landmarks. Anterior and posterior cytoarchitectonic borders also do not show a reliable association with macroanatomical landmarks. Moreover, comparisons of the Talairach coordinates of the transverse sulci and those of the borders of Te1 show significant discrepancies between

TABLE 3

Relative Laminar Cell Volume Densities of Cortical Layers ± SD (GLI%)

	Left			Right		
Layer	Te 1.2	Te 1.0	Te 1.1	Te 1.2	Te 1.0	Te 1.1
II	21.3 ± 2.8	24.4 ± 4.7	24.5 ± 3.3	22.3 ± 2.8	22.1 ± 3.5	22.5 ± 3.9
III	20.4 ± 2.6	23.4 ± 4.4	23.3 ± 3.4	21.2 ± 2.1	21.1 ± 3.3	20.9 ± 3.8
IV	21.7 ± 2.7	24.8 ± 4.6	25.1 ± 3.4	23.1 ± 2.1	22.3 ± 3.0	22.4 ± 3.8
V	20.2 ± 2.7	22.7 ± 4.3	22.5 ± 2.9	21.3 ± 2.0	20.7 ± 2.9	20.4 ± 3.5
VI	19.9 ± 2.9	22.8 ± 4.2	22.0 ± 2.9	20.9 ± 2.1	20.1 ± 3.1	19.8 ± 3.4

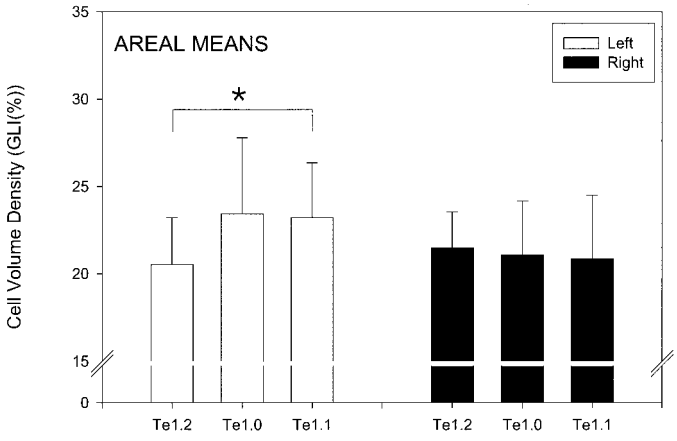

FIG. 6. Means and standard deviations of cell volume density (GLI(%)) in areas Te1.2, Te1.0, and Te1.1 calculated from 10 left and 10 right hemispheres. The significant difference is marked by an asterisk.

both markers, which cannot be predicted a priori by inspection of the gross morphology (Fig. 10).

Figure 11 shows a map of Te1 of one brain with its three subdivisions as an example of the cytoarchitectonic mapping to the MRI representation of the standard reference brain.

DISCUSSION

In contrast to classical cytoarchitectonic observations which rely on visual inspection of histological sections (Brodmann, 1909; Economo and Koskinas, 1925), the present cytoarchitectonic study is based on an observer-independent method for the detection of areal borders and quantification of cytoarchitectonic variability (Amunts *et al.*, 1999). This approach permits statistical testing of the significance of areal borders and does not depend on individual pattern recognition abilities necessary for the classical method. The definition of borders by the novel technique is based on the statistical analysis of multivariate distance functions analogous to statistics in functional brain imaging studies in which significant activations are revealed by statistical parametric mapping (Friston *et al.*, 1996). This architectonic technique has recently been applied to the analysis of the primary motor, somatosensory, and visual cortices as well as Broca's region (Geyer *et al.*, 1996, 1999; Amunts *et al.*, 1999, 2000). The major aspects of cytoarchitectonic organization are represented by cell body volume density (GLI) profiles. Since the GLI profiles, registered in distinct cortical areas, are architectonic "fingerprints" of the respective area (Hudspeth *et al.*, 1976), laminar cell density and layer thickness can be extracted and statistically tested for gender-, side-, and area-dependent heterogeneity.

Noninvasive functional brain mapping of the human auditory system needs a precise and reliable architectonic map for the anatomical interpretation of activation clusters after auditory stimulation. The present study demonstrates sharp borders of the putative functional primary auditory cortex, the koniocortical region Te1, that were in good agreement with results obtained by pure visual inspection for Brodmann's area 41 (Brodmann, 1909) and von Economo's and Koskinas' (1925) areas TC and TD as far as the topography can be derived from the 2-D schematic drawings of these publications. Moreover, the observer-independent detection of cytoarchitectonic borders reveals a significant architectonical heterogeneity of the primary auditory cortex Te1. Three statistically distinct cytoarchitectonic areas, i.e., areas Te1.2, Te1.0, and Te1.1, can be localized for the first time in the medial-to-lateral direction. While only subtle changes in the laminar patterns are recognizable, which are difficult to localize by pure visual inspection, quantitative analysis of the cytoarchitecture provides reliable areal borders in all 10

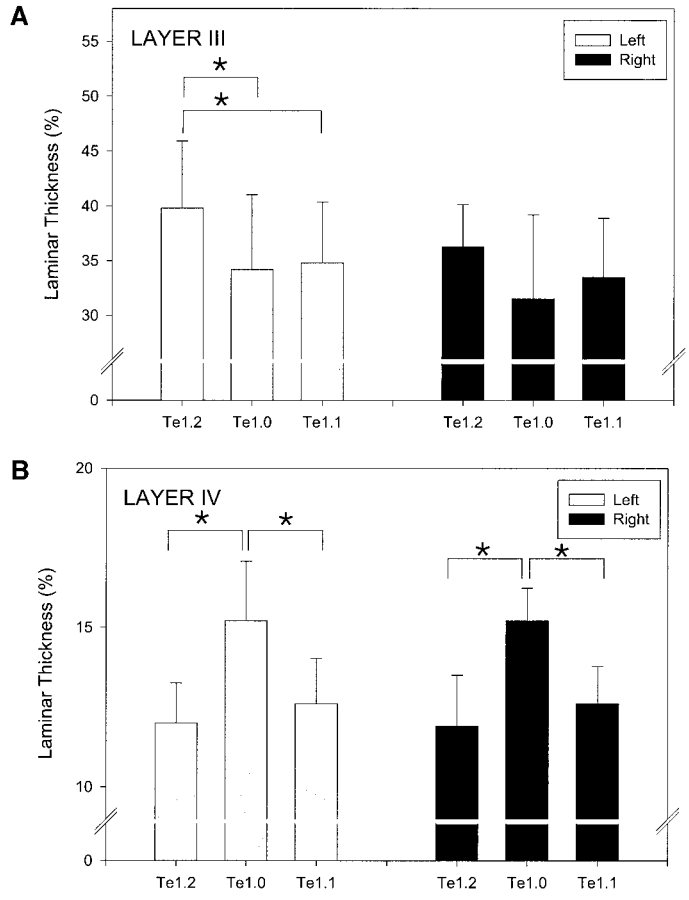

FIG. 7. Mean and standard deviation of relative laminar thickness (%) in areas Te1.2, Te1.0, and Te1.1 calculated from 10 left and 10 right hemispheres. (A) Laminar thickness of layer III. (B) Laminar thickness of layer IV. Significant differences are marked by asterisks.

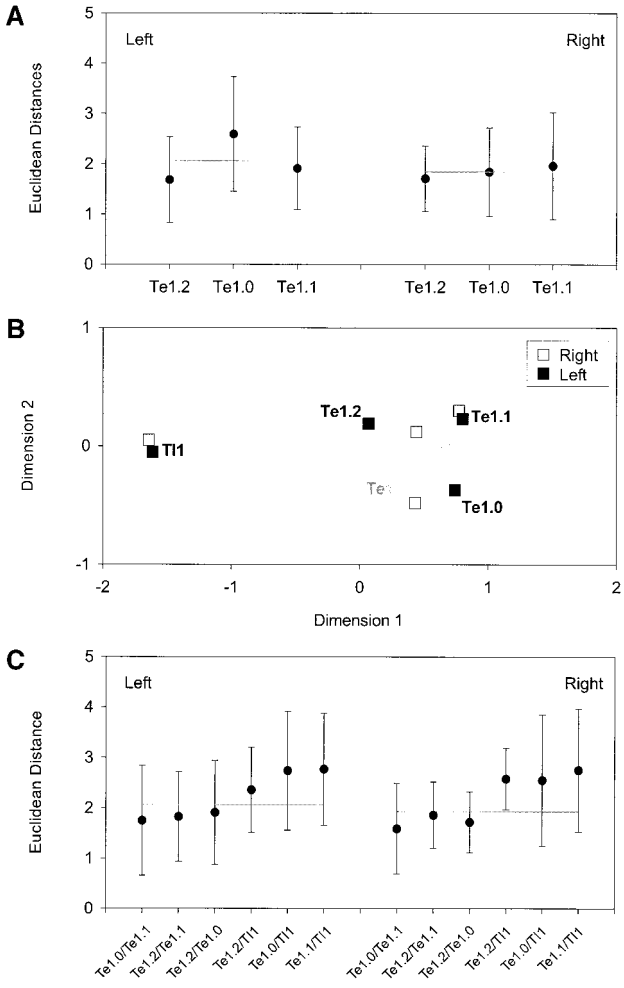

FIG. 8. (A) Means and standard deviations of intersubject distances. Euclidean distances between the GLI profiles of all possible unique pairs (n = 45 distances for each area in each hemisphere) of corresponding areas (Te1.2, Te1.1, or Te1.0) in the left or right hemispheres of 10 brains were calculated and averaged; black lines indicate the grand average distance (in this example, average of the mean intersubject differences of all three primary auditory areas). (B) Interareal distances between primary auditory areas Te1.2, Te1.0, and Te1.1 and one neighboring nonprimary area TI1 after multidimensional scaling (for details see Results). Calculations were made separately for each side; for visualization, the results from both sides are depicted in the same graph. The three primary auditory areas of the left and right hemispheres show lower mutual distances than each of them with the nonprimary area TI1. Thus, Te1.0, Te1.1, and Te1.2 comprise a family of architectonically nearly related areas (i.e., the areas of the primary auditory cortex Te1), although they differ significantly in their laminar patterns as shown in Figs. 3, 5, and 6. (C) Means and standard deviations of interareal Euclidean distances between primary auditory areas Te1.2, Te1.0, Te1.1, and the neighboring nonprimary area TI1; black lines represent the grand average intersubject distances in the left and right hemispheres.

brains analyzed. The three primary auditory areas are mapped to a spatial reference system, i.e., the standard brain (see Materials and Methods). This step is a prerequisite for generating population maps of the human primary auditory cortex and its areas (see companion article by J. Rademacher *et al.*). The question of whether activation clusters are related to specific structural entities can be answered only if such architectonically defined borders have been defined.

Areas Te1.2, Te1.0, and Te1.1 share the typical features of a primary sensory cortical area, i.e., small granular cells across the entire cortical ribbon, relatively small pyramidal cells in layer IIIc, a prominent width of layer IV, and a relative cell-sparse layer V (Economo and Koskinas, 1925; Galaburda and Sanides, 1980; Rademacher *et al.*, 1993). Quantitative comparisons of laminar thickness reveal significant interareal differences for the thickness of layers III and IV. Granular layer IV is widest in area Te1.0, which also shows the highest density of granular cells compared with other cortical layers. Thus, we interpret area Te1.0 as the koniocortical core field. The layer-

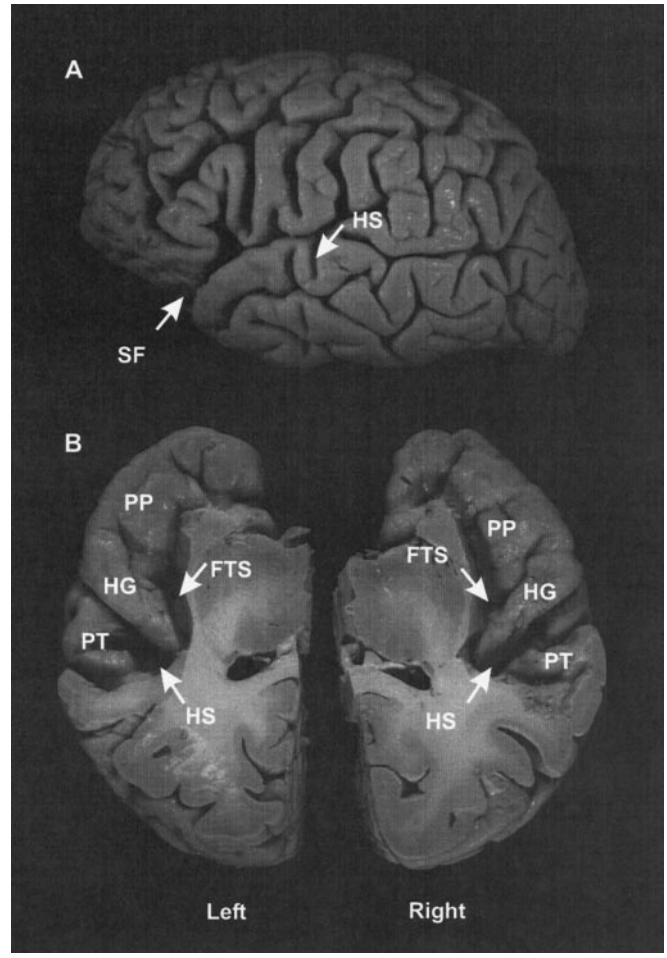

FIG. 9. An individual brain (SN 519/79, not included in our sample) showing macroanatomical landmarks of the primary auditory region. (A) Lateral view. (B) Dorsal view after removal of the frontal and parietal opercula. SF, Sylvian fissure; FTS, first transverse temporal sulcus; HS, Heschl's sulcus; HG, Heschl's gyrus; PP, planum polare; PT, planum temporale.

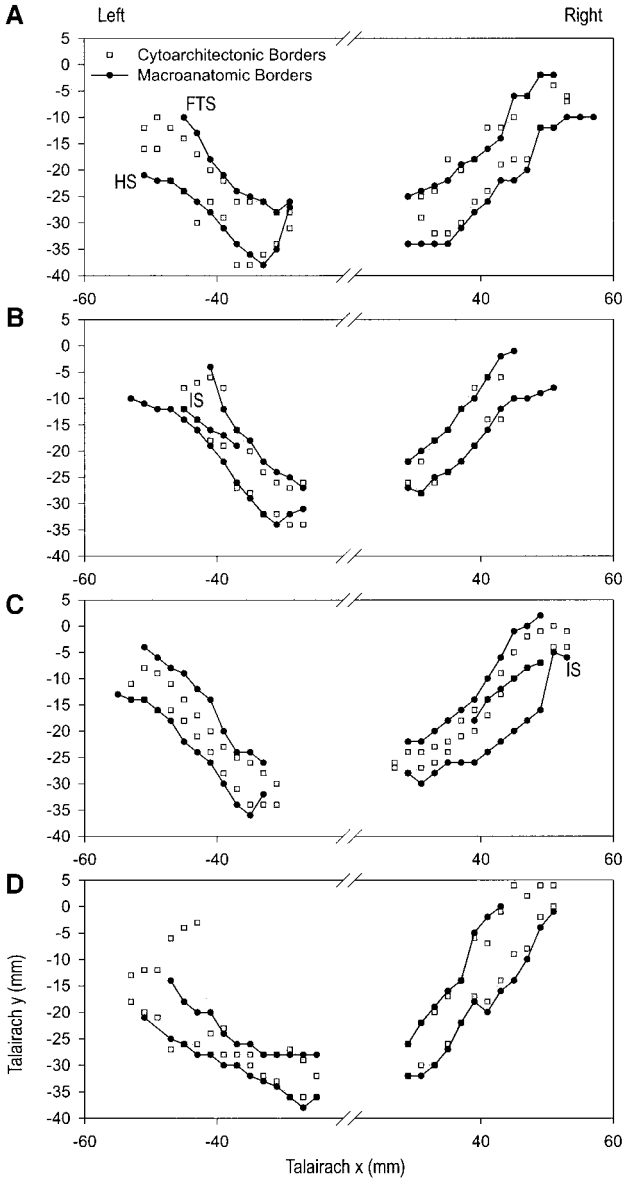

FIG. 10. Graphical representation of the relationship between Talairach coordinates of brain sulci and cytoarchitectonic borders of region Te1 in four brains (A–D) of the present sample. Discrepancies between cytoarchitectonic borders and macroscopical landmarks are clearly visible and vary from brain to brain and between hemispheres. FTS, first transverse temporal sulcus; HS, Heschl's sulcus; IS, intermediate sulcus.

specific interareal differences are probably indicating quantitative differences in thalamocortical projections between the three primary auditory areas, since layer IV is the major target of the ascending projections from the medial geniculate body. Medial area Te1.1 and lateral area Te1.2 are less granular than area Te1.0.

While this subdivision of Te1 into three areas is in contrast to Brodmann's map (1909), other subparcellations of the primary auditory cortex have been reported. Areas TC and TD of von Economo and Koskinas (1925) and areas Kam and Kalt of Galaburda and Sanides (1980) were recognized in the medial-to-lateral direction on HG. Others have found much more extensive cytoarchitectonic subparcellations of the primary auditory areas with up to 11 types of granular cortices located on HG (Economo and Horn, 1930). However, these extensive parcellations could not be reproduced by us. It remains questionable whether they are consistently and reliably demonstrable cortical entities in a sample of different human brains. However, a consistent aspect of all these cytoarchitectonic maps is the description of a core region which has a more granular appearance than the remaining PAC. This region is comparable to area Te1.0. Medially neighboring areas have been characterized by the "fogging" of the cortical layering and by the occurrence of medium-sized pyra-

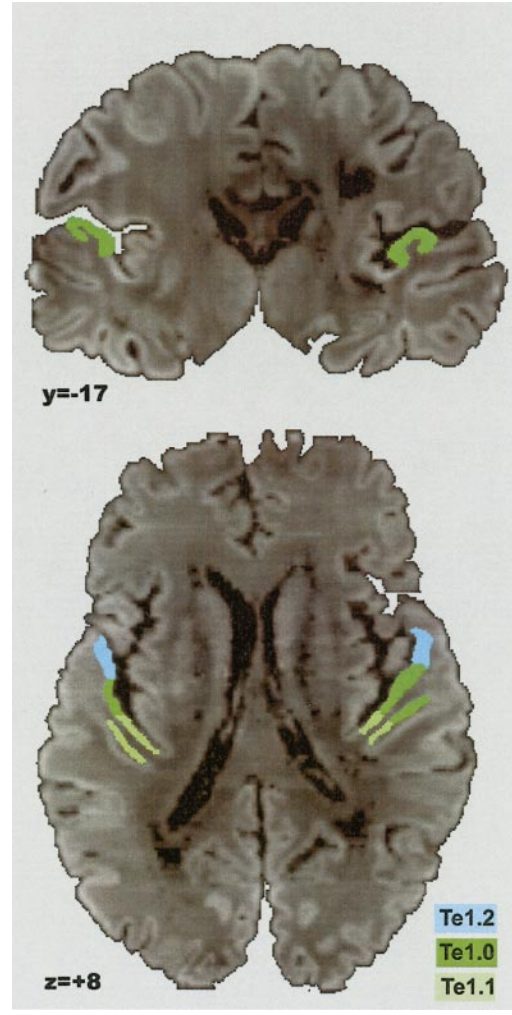

FIG. 11. Maps of areas Te1.2, Te1.0, and Te1.1 in a coronal (top) and horizontal (bottom) histological section (gray values of the histological sections are inverted) after spatial normalization to the corresponding postmortem MRI. Sections of an individual brain are shown as an example. Using the human brain atlas, corresponding Talairach coordinates have been calculated (Roland and Zilles, 1994, 1998).

midal cells. These features are characteristic of our area Te1.1. The cytoarchitectonic region at the lateral border of HG—area TBC of von Economo and Koskinas (1925)—was described as a transitional zone between the primary auditory and the nonprimary areas. This area resembles area Te1.2 in the present study.

This brief discussion shows also that comparisons between previous studies is difficult, because of observer-dependent, nonquantitative criteria (Zilles, 1990) and the lack of spatial normalization procedures used in these studies. The major advantage of the present approach is that our maps can be easily compared with any future quantitative cytoarchitectonic study in a common spatial reference system. Moreover, the method of observer-independent localization of areal borders can also be applied to myeloarchitectonic and receptor architectonic studies offering a multimodal characterization of cortical architecture (Roland and Zilles, 1994). Several examples of a combined cyto- and receptor-architectonic approach demonstrate the effectiveness of this approach (Zilles *et al.,* 1995; Geyer *et al.,* 1996; Roland and Zilles, 1996). For the organization of the human primary auditory cortex, this approach will introduce new aspects, since indications of multimodal heterogeneity were already brought up from myeloarchitectonic (Beck, 1930; Hopf, 1954), pigmentoarchitectonic (Braak, 1978), acetylcholinesterase (Hutsler and Gazzaniga, 1996; Rivier and Clarke, 1997), and cytochromoxidase studies (Rivier and Clarke, 1997; Clarke and Rivier, 1998).

The functional meaning of the three primary auditory areas is not known. Electrophysiologic studies of the human supratemporal cortex have demonstrated evoked potentials with shorter amplitudes and higher latencies within than outside PAC. A recent study (Liegeois Chauvel *et al.,* 1994) differentiated several components of intracerebral middle latency auditory-evoked potentials (MLAEPs; N30, P50, N60, N75) which were generated in HG with different topographies along the gyrus. N30 is generated in the medial and P50 in the central part of HG, both activations being interpreted as responses of the primary auditory cortex to tone burst. The generator sources of N60 and N75 are located in the lateral part of HG. Neuromagnetic measurements of the primary auditory response confirmed the existence of several generator sources along HG (Yoshiura *et al.,* 1995). Considering the different latencies of the MLAEPS along the mediolateral axis of HG, medially located area Te1.1 may correspond to the generator source of the early MLAEPs, area Te1.0 to the generator source of the middle MLAEPs, and area Te1.2 to the generator source of the late MLAEPs. A tonotopic organization of the PAC with high frequencies being represented posteromedially and low frequencies anterolaterally has been demonstrated using magnetoencephalography (Romani *et al.,* 1982b; Tiitinen *et al.,* 1993; Pantev *et al.,* 1995; Verkindt *et al.,* 1995), intracerebral electrophysological recordings (Howard *et al.,* 1996), and functional imaging (Lauter *et al.,* 1985; Talavage *et al.,* 1996; Bilecen *et al.,* 1998). Posteromedial activity would probably map onto area Te1.1 and anterolateral activity would relate to area Te1.2. Centrally located area Te1.0 would then relate to those frequencies which characterize human speech. Recent functional imaging studies of foreground–background decomposition of auditory perception cortex show two field-specific activations of HG, T1a and T1b (Scheich *et al.,* 1998). These foci of activation probably map on the combined areas Te1.1 and Te1.0 (T1b) and on area Te1.2 (T1a).

Intersubject variability in cytoarchitecture of cortical areas was repeatedly described (Economo and Horn, 1930; Bailey and von Bonin, 1951). Since this may obscure cytoarchitectonic differences between cortical areas, Lashley and Clark (1946) questioned practically all previous cytoarchitectonic attempts of cortical parcellations. Thus, we measured interareal and intersubject variabilities of the auditory areas and compared both parameters. As predicted in the literature, the laminar patterns of each of the primary auditory areas showed a considerable variability between subjects. The highest variability was seen in left area Te1.0. This will obscure cytoarchitectonic differences between areas Te1.2, Te1.0, and Te1.1, if GLI profiles are averaged across all brains, but does not prevent parcellation based on GLI profiles for defining the areal borders in each brain. The generalized criticism of cytoarchitectonic analyses by Lashley and Clark (1946) is, therefore, not justified.

Moreover, the present study of the auditory cortex demonstrates larger cytoarchitectonic differences between cortical regions related to different hierarchical levels (i.e., Te1 versus TI1) within a sensory system and relatively small differences between areas belonging to the same hierarchical level (i.e., areas Te1.1, Te1.0, and Te1.2 of the whole primary auditory cortex Te1).

The cytoarchitectonic variability of the laminar organization is accompanied by a topographic variability of the areal borders of Te1.2, Te1.0, and Te1.0 relative to macroanatomical landmarks. This finding is paralleled by a similar variability found in Broca's region (Amunts *et al.,* 1999) and in the visual cortex (Amunts *et al.,* 2000). Although the primary auditory areas are found consistently on HG in the depth of the Sylvian fissure (class II variability of Rademacher *et al.,* 1993), the cytoarchitectonic *borders* of the Te1 region did not perfectly match the macroanatomical geometry of Heschl's transverse gyrus (class I variability of Rademacher *et al.,* 1993). The same cytoarchitectonic border could be localized either in the depth of the transverse sulcus or at the crown of the transverse gyrus depending on the individual case. Even more striking, the lateral border of Te1 can be found entirely on HG in

some cases, but extend onto the neighboring superior temporal cortex in other cases. There are no macroscopic features which indicate consistently a cytoarchitectonic border.

The reason for this dissociation of cytoarchitectonic borders and reliable sulcal landmarks (cf. Fig. 11) is not known, but it is tempting to speculate about epigenetic influences on the growth of specific cortical areas in different subjects. Cytoarchitectonic and topographic variability of cortical areas is shaped by interaction of genetic and environmental factors as described for the visual cortex (Hubel and Wiesel, 1977; Rakic, 1991). The influences of training, experience, and early phonetic environment were recently studied in primate and human auditory cortex (Rauschecker, 1999). In humans, macroanatomical variations of HG visualized by *in vivo* magnetic resonance imaging were interpreted as anatomical substrates of behavioral variations. Furthermore, it has been reported that the frequency of duplicated Heschl gyri is increased in families with learning disabilities (Leonard *et al.*, 1995). Finally, there are hints as to the impact of early musical training on the development of absolute pitch and a concomitant expansion of the auditory cortex (Schlaug *et al.*, 1995; Pantev *et al.*, 1998b). Such genetic and/or epigenetic phenomena point to hitherto unknown complex and differential influences of auditory function on the expression of gyral and cytoarchitectonic patterns.

In contrast to a large number of reports on interhemispheric asymmetries in the human language areas including the planum temporale (Geschwind and Levitsky, 1968; Steinmetz *et al.*, 1990; Witelson and Kigar, 1992; Jacobs *et al.*, 1993; Schlaug *et al.*, 1995) and cytoarchitectonic area Tpt (Galaburda *et al.*, 1978), such asymmetries have only rarely been analyzed in the auditory system where a leftward asymmetry of cortex (Rademacher *et al.*, 1993) and white matter fiber tracts (Penhune *et al.*, 1996) may be present in more than half of all brains. Golgi studies of the primary auditory cortex have shown larger cortical columns on the left side with longer distances between columns and greater dendritic arborization (Seldon, 1981). In the present paper, we report left–right differences in volume fraction of cell bodies in the primary auditory areas Te1.1, Te1.0, and Te1.2. In areas Te1.1 and Te1.0, cell volume fractions were consistently higher in the left than in the right hemisphere, while the opposite relation (right $>$ left) was found in area Te1.2. Significantly higher cell volume densities were found in Te1.1 compared to Te1.2 in the left, but not in the right, hemisphere. Such left–right asymmetry of GLI reflects a higher number of neurons per unit volume in the hemisphere with the higher GLI values (Wree *et al.*, 1982). One may speculate that leftward asymmetries of neuronal density in Te1.0 and Te1.1 may represent an anatomical substrate for language lateralization (Geschwind and Galaburda, 1985). Similar differences in numerical density of neurons in posterior temporal cortex between men and women have been proposed as the morphological substrate for gender differences in cognition, behavior, and language lateralization (Hier *et al.*, 1994; Witelson *et al.*, 1995; Shaywitz *et al.*, 1995). In contrast to the significant interhemispheric differences in GLI, we did not observe gender differences in GLI or laminar thickness in Te1.

In conclusion, the observer-independent method enables the delineation of three primary auditory areas, Te1.1, Te1.0, and Te1.2, in the human brain. The intrasubject cytoarchitectonic differences between these primary auditory areas are significant, but lower than the intersubject variability of each of these areas. The cytoarchitectonic differences between the primary auditory areas and a neighboring nonprimary area, TI1, exceed intersubject variability. We demonstrate that the borders of Te1 cannot be reliably and precisely localized on the basis of macroanatomic landmarks and thus also not on the basis of individual magnetic resonance imaging. There are no sulcal landmarks for their medial-to-lateral topography of the three areas. Since for the time being, precise and exact cytoarchitectonic parcellation cannot be made in living brains, we have presented a postmortem anatomical analysis of PAC, which provides the cytoarchitectonic detail needed for structural–functional comparisons. It takes into account interhemispheric and intersubject differences at the architectonic level. Furthermore, it provides a basis for further studies of topographic variability of PAC (see companion article by J. Rademacher *et al.*). The present anatomic mapping of PAC provides both a revision of the classical cytoarchitectonic maps and a computational methodology for its integration with structural or functional 3-D data sets from other studies. Such a system will allow one to colocalize a specifically activated area with a distinct cytoarchitectonic area (Roland and Zilles, 1994, 1996, 1998; Mazziotta *et al.*, 1995; Geyer *et al.*, 1996; Amunts *et al.*, 1999, 2000; Larsson *et al.*, 1999; Naito *et al.*, 1999; Bodegård *et al.*, 2000a,b).

ACKNOWLEDGMENTS

This work was supported by grants from the DFG, SFB 194/A6, and the "Human Brain Project," MH52176P01. The authors thank Christine Opfermann-Rüngeler and Uli Bürgel for their technical assistance and Ursula Blohm and Brigitte Machus for preparing the histological material.

REFERENCES

Amunts, K., Schleicher, A., Burgel, U., Mohlberg, H., Uylings, H. B. M., and Zilles, K. 1999. Broca's region revisited: Cytoarchitecture and intersubject variability. *J. Comp. Neurol.* **412:** 319–341.

Amunts, K., Malikovic, A., Mohlberg, H., Schormann, T., and Zilles, K. 2000. Brodmann's areas 17 and 18 brought into stereotaxic space—Where and how variable? *NeuroImage* **11:** 66–84.

Bailey, P., and von Bonin, G. 1951. *The Isocortex of Man*. Univ. of Illinois Press, Urbana.

Beck, E. 1930. Die Myeloarchitektonik der dorsalen Schläfenlappenrinde beim Menschen. *J. Psychol. Neurol.* **41:** 129–263.

Belin, P., Zilbovicius, M., Crozier, S., Thivard, L., Fontaine, A., Masure, M. C., and Samson, Y. 1998. Lateralization of speech and auditory temporal processing. *J. Cognit. Neurosci.* **10:** 536–540.

Bilecen, D., Scheffler, K., Schmid, N., Tschopp, K., and Seelig, J. 1998. Tonotopic organization of the human auditory cortex as detected by BOLD-fMRI. *Hear. Res.* **126:** 19–27.

Binder, J. R., Rao, S. M., Hammeke, T. A., Yetkin, F. Z., Jesmanowicz, A., Bandettini, P. A., Wong, E. C., Estkowski, L. D., Goldstein, M. D., Haughton, V. M., *et al.* 1994. Functional magnetic resonance imaging of human auditory cortex. *Ann. Neurol.* **35:** 662–672.

Bodegård, A., Geyer, S., Naito, E., Zilles, K., and Roland, P. E. 2000a. Somatosensory areas in man activated by moving stimuli: Cytoarchitectonic mapping and PET. *NeuroReport* **11:** 187–191.

Bodegård, A., Ledberg, A., Geyer, S., Naito, E., Larsson, J., Zilles, K., and Roland, P. E. 2000b. Object shape differences reflected by somatosensory cortical activation. *J. Neurosci.* **20:** 1–5.

Braak, H. 1978. The pigment architecture of the human temporal lobe. *Anat. Embryol. Berlin* **154:** 213–240.

Brodmann, K. 1909. *Vergleichende Lokalisationslehre der Grosshirnrinde in Ihren Prinzipien Dargestellt auf Grund des Zellaufbaus.* Barth, Leipzig.

Castleman, K. R. 1979. *Digital Image Processing.* Prentice Hall, Englewood Cliffs, NJ.

Celesia, G. G. 1976. Organization of auditory cortical areas in man. *Brain* **99:** 403–414.

Clarke, S., and Rivier, F. 1998. Compartments within human primary auditory cortex: Evidence from cytochrome oxidase and acetylcholinesterase staining. *Eur. J. Neurosci.* **10:** 741–745.

Dixon, W. J., Brown, M. B., Engelman, L., Hill, M. A., and Jennrich, R. I. 1988. *BMDP Statistical Software Manual.* Univ. of California Press, Berkley.

Economo, C., and Koskinas, G. N. 1925. *Die Cytoarchitektonik der Hirnrinde des Erwachsenen Menschen.* Springer-Verlag, Berlin.

Economo, C., and Horn, L. 1930. Über Windungsrelief, Masse und Rindenarchitectonik der Supratemporalfläche, ihre individuellen und ihre Seitenunterschiede. *Z. Neurol. Psychiat.* **130:** 678–757.

Friston, K. J., Holmes, A., Poline, J. B., Price, C. J., and Frith, C. D. 1996. Detecting activations in PET and fMRI: Levels of inference and power. *NeuroImage* **4:** 223–235.

Galaburda, A. M., Sanides, F., and Geschwind, N. 1978. Human brain: Cytoarchitectonic left–right asymmetries in the temporal speech region. *Arch. Neurol.* **35:** 812–817.

Galaburda, A., and Sanides, F. 1980. Cytoarchitectonic organization of the human auditory cortex. *J. Comp. Neurol.* **190:** 597–610.

Geschwind, N., and Levitsky, W. 1968. Human brain: Left–right asymmetries in temporal speech region. *Science* **161:** 186–187.

Geschwind, N., and Galaburda, A. M. 1985. Cerebral lateralization: Biological mechanisms, associations, and pathology. I. A hypothesis and a program for research. *Arch. Neurol.* **42:** 428–459.

Geyer, S., Ledberg, A., Schleicher, A., Kinomura, S., Schormann, T., Burgel, U., Klingberg, T., Larsson, J., Zilles, K., and Roland, P. E. 1996. Two different areas within the primary motor cortex of man. *Nature* **382:** 805–807.

Geyer, S., Schleicher, A., and Zilles, K. 1999. Areas 3a, 3b, and 1 of human primary somatosensory cortex. *NeuroImage* **10:** 63–83.

Hari, R. 1991. Activation of the human auditory cortex by speech sounds. *Acta Otolaryngol. Suppl. Stockholm* **491:** 132–138.

Hari, R., Hamalainen, M., Ilmoniemi, R., Kaukoranta, E., Reinikainen, K., Salminen, J., Alho, K., Naatanen, R., and Sams, M. 1984. Responses of the primary auditory cortex to pitch changes in a sequence of tone pips: Neuromagnetic recordings in man. *Neurosci. Lett.* **50:** 127–132.

Henery, R. J., Robinson, J., and Bennett, M. R. 1998. Methods for grouping shapes of synaptic current recorded from sets of synapses. *J. Neurosci. Methods* **86:** 79–90.

Hier, D. B., Yoon, W. B., Mohr, J. P., Price, T. R., and Wolf, P. A. 1994. Gender and aphasia in the Stroke data bank. *Brain Lang.* **47:** 155–167.

Hopf, A. 1954. Die Myeloarchitektonik des Isokortex temporalis beim Menschen. *J. Hirnforsch.* **1:** 208–279.

Howard, M. A., Volkov, I. O., Abbas, P. J., Damasio, H., Ollendieck, M. C., and Granner, M. A. 1996. A chronic microelectrode investigation of the tonotopic organization of human auditory cortex. *Brain Res.* **724:** 260–264.

Hubel, D. H., and Wiesel, T. N. 1977. Ferrier lecture. Functional architecture of macaque monkey visual cortex. *Proc. R. Soc. London B Biol. Sci.* **198:** 1–59.

Hudspeth, A. J., Ruark, J. E., and Kelly, J. P. 1976. Cytoarchitectonic mapping by microdensitometry. *Proc. Natl. Acad. Sci. USA* **73:** 2928–2931.

Hutsler, J. J., and Gazzaniga, M. S. 1996. Acetylcholinesterase staining in human auditory and language cortices: Regional variation of structural features. *Cereb. Cortex* **6:** 260–270.

Iwamura, Y., Iriki, A., and Tanaka, M. 1994. Bilateral hand representation in the postcentral somatosensory cortex. *Nature* **369:** 554–556.

Jacobs, B., Schall, M., and Scheibel, A. B. 1993. A quantitative dendritic analysis of Wernicke's area in humans. II. Gender, hemispheric, and environmental factors. *J. Comp. Neurol.* **327:** 97–111.

Kaas, J. H., Nelson, R. J., Sur, M., Lin, C. S., and Merzenich, M. M. 1979. Multiple representations of the body within the primary somatosensory cortex of primates. *Science* **204:** 521–523.

Langner, G., Sams, M., Heil, P., and Schulze, H. 1997. Frequency and periodicity are represented in orthogonal maps in the human auditory cortex: Evidence from magnetoencephalography. *J. Comp. Physiol. A* **181:** 665–676.

Larsson, J., Amunts, K., Gulyas, B., Malikovic, A., Zilles, K., and Roland, P. E. 1999. Neuronal correlates of real and illusory contour perception: Functional anatomy with PET. *Eur. J. Neurosci.* **11:** 4024–4036.

Lashley, K. S., and Clark, G. 1946. The cytoarchitecture of the cerebral cortex of Ateles: A critical examination of architectonic studies. *J. Comp. Neurol.* **85:** 223–305.

Lauter, J. L. 1992. Processing asymmetries for complex sounds: Comparisons between behavioral ear advantages and electrophysiological asymmetries based on quantitative electroencephalography. *Brain Cognit.* **19:** 1–20.

Lauter, J. L., Herscovitch, P., Formby, C., and Raichle, M. E. 1985. Tonotopic organization in human auditory cortex revealed by positron emission tomography. *Hear. Res.* **20:** 199–205.

Leonard, C. M., Martinez, P., Weintraub, B. D., and Hauser, P. 1995. Magnetic resonance imaging of cerebral anomalies in subjects with resistance to thyroid hormone. *Am. J. Med. Genet.* **60:** 238–243.

Leonard, C. M., Puranik, C., Kuldau, J. M., and Lombardino, L. J. 1998. Normal variation in the frequency and location of human auditory cortex landmarks. Heschl's gyrus: Where is it? *Cereb. Cortex* **8:** 397–406.

Liegeois Chauvel, C., Musolino, A., and Chauvel, P. 1991. Localization of the primary auditory area in man. *Brain* **114:** 139–151.

Liegeois Chauvel, C., Musolino, A., Badier, J. M., Marquis, P., and Chauvel, P. 1994. Evoked potentials recorded from the auditory cortex in man: Evaluation and topography of the middle latency components. *Electroencephalogr. Clin. Neurophysiol.* **92:** 204–214.

Matsumiya, Y., Tagliasco, V., Lombroso, C. T., and Goodglass, H. 1972. Auditory evoked response: Meaningfulness of stimuli and interhemispheric asymmetry. *Science* **175:** 790–792.

Mazziotta, J. C., Toga, A. W., Evans, A., Fox, P., and Lancaster, J. 1995. A probabilistic atlas of the human brain: Theory and rationale for its development. The International Consortium for Brain Mapping (ICBM). *NeuroImage* **2:** 89–101.

McFadden, D. 1993. A speculation about the parallel ear asymmetries and sex differences in hearing sensitivity and otoacoustic emissions. *Hear. Res.* **68:** 143–151.

Merker, B. 1983. Silver staining of cell bodies by means of physical development. *J. Neurosci. Methods* **9:** 235–241.

Merzenich, M. M., Kaas, J. H., Sur, M., and Lin, C. S. 1978. Double representation of the body surface within cytoarchitectonic areas 3b and 1 in "SI" in the owl monkey (Aotus trivirgatus). *J. Comp. Neurol.* **181:** 41–73.

Naito, E., Ehrsson, H. H., Geyer, S., Zilles, K., and Roland, P. E. 1999. Illusory arm movements activate cortical motor areas: A positron emission tomography study. *J. Neurosci.* **19:** 6134–6144.

Nicholls, M. E. 1998. Support for a structural model of aural asymmetries. *Cortex* **34:** 99–110.

Ottaviani, F., Di Girolamo, S., Briglia, G., De Rossi, G., Di Giuda, D., and Di Nardo, W. 1997. Tonotopic organization of human auditory cortex analyzed by SPET. *Audiology* **36:** 241–248.

Pantev, C., Hoke, M., Lehnertz, K., and Lutkenhoner, B. 1989a. Neuromagnetic evidence of an amplitopic organization of the human auditory cortex. *Electroencephalogr. Clin. Neurophysiol.* **72:** 225–231.

Pantev, C., Hoke, M., Lutkenhoner, B., and Lehnertz, K. 1989b. Tonotopic organization of the auditory cortex: Pitch versus frequency representation. *Science* **246:** 486–488.

Pantev, C., Bertrand, O., Eulitz, C., Verkindt, C., Hampson, S., Schuierer, G., and Elbert, T. 1995. Specific tonotopic organizations of different areas of the human auditory cortex revealed by simultaneous magnetic and electric recordings. *Electroencephalogr. Clin. Neurophysiol.* **94:** 26–40.

Pantev, C., Ross, B., Berg, P., Elbert, T., and Rockstroh, B. 1998a. Study of the human auditory cortices using a whole-head magnetometer: Left vs. right hemisphere and ipsilateral vs. contralateral stimulation. *Audiol. Neurootol.* **3:** 183–190.

Pantev, C., Oostenveld, R., Engelien, A., Ross, B., Roberts, L. E., and Hoke, M. 1998b. Increased auditory cortical representation in musicians. *Nature* **392:** 811–814.

Penhune, V. B., Zatorre, R. J., MacDonald, J. D., and Evans, A. C. 1996. Interhemispheric anatomical differences in human primary auditory cortex: Probabilistic mapping and volume measurement from magnetic resonance scans. *Cereb. Cortex* **6:** 661–672.

Pfeifer, R. A. 1920. Myelogenetisch-anatomische Untersuchungen ueber das kortikale Ende der Hoerleitung. *Abh. Math. Phys. Saech. Akad. Wiss.* **37:** 1–54.

Poeppel, D., Yellin, E., Phillips, C., Roberts, T. P., Rowley, H. A., Wexler, K., and Marantz, A. 1996. Task-induced asymmetry of the auditory evoked M100 neuromagnetic field elicited by speech sounds. *Brain Res. Cognit. Brain Res.* **4:** 231–242.

Polyakov, A., and Pratt, H. 1995. Three-channel Lissajous' trajectory of the binaural interaction components of human auditory middle-latency evoked potentials. *Hear. Res.* **82:** 205–215.

Rademacher, J., Caviness, V. S., Jr., Steinmetz, H., and Galaburda, A. M. 1993. Topographical variation of the human primary cortices: Implications for neuroimaging, brain mapping, and neurobiology. *Cereb. Cortex* **3:** 313–329.

Rajkowska, G., and Goldman-Rakic, P. S. 1995. Cytoarchitectonic definition of prefrontal areas in the normal human cortex. I. Remapping of areas 9 and 46 using quantitative criteria. *Cereb. Cortex* **5:** 307–322.

Rakic, P. 1991. Experimental manipulation of cerebral cortical areas in primates. *Philos. Trans. R. Soc. London B Biol. Sci.* **331:** 291–294.

Rauschecker, J. P. 1999. Auditory cortical plasticity: A comparison with other sensory systems. *Trends Neurosci.* **22:** 74–80.

Reite, M., Zimmerman, J. T., and Zimmerman, J. E. 1981. Magnetic auditory evoked fields: Interhemispheric asymmetry. *Electroencephalogr. Clin. Neurophysiol.* **51:** 388–392.

Reite, M., Zimmerman, J. T., and Zimmerman, J. E. 1982. MEG and EEG auditory responses to tone, click and white noise stimuli. *Electroencephalogr. Clin. Neurophysiol.* **53:** 643–651.

Reite, M., Adams, M., Simon, J., Teale, P., Sheeder, J., Richardson, D., and Grabbe, R. 1994. Auditory M100 component 1: Relationship to Heschl's gyri. *Brain Res. Cognit. Brain Res.* **2:** 13–20.

Rivier, F., and Clarke, S. 1997. Cytochrome oxidase, acetylcholinesterase, and NADPH-diaphorase staining in human supratemporal and insular cortex: Evidence for multiple auditory areas. *NeuroImage* **6:** 288–304.

Roland, P. E., and Zilles, K. 1994. Brain atlases—A new research tool. *Trends Neurosci.* **17:** 458–467.

Roland, P. E., and Zilles, K. 1996. The developing European computerized human brain database for all imaging modalities. *NeuroImage* **4:** S39–47.

Roland, P. E., and Zilles, K. 1998. Structural divisions and functional fields in the human cerebral cortex. *Brain Res. Brain Res. Rev.* **26:** 87–105.

Romani, G. L., Williamson, S. J., Kaufman, L., and Brenner, D. 1982a. Characterization of the human auditory cortex by the neuromagnetic method. *Exp. Brain Res.* **47:** 381–393.

Romani, G. L., Williamson, S. J., and Kaufman, L. 1982b. Tonotopic organization of the human auditory cortex. *Science* **216:** 1339–1340.

Sarkissov, S. A., Filimonoff, I. N., Kononowa, I. P., Preobrazeanskaja, N. S., and Kukuewa, L. A. 1955. *Atlas of the Cytoarchitectonics of the Human Cerebral Cortex.* Medgiz, Moscow. [In Russian]

Scheich, H., Baumgart, F., Gaschler-Markefski, B., Tegeler, C., Tempelmann, C., Heinze, H. J., Schindler, F., and Stiller, D. 1998. Functional magnetic resonance imaging of a human auditory cortex area involved in foreground–background decomposition. *Eur. J. Neurosci.* **10:** 803–809.

Scheuneman, D., Teale, P., Linnville, S., Goldstein, L., and Reite, M. 1991. Magnetic auditory M100 source location in normal females. *Brain Res. Bull.* **26:** 747–751.

Schlaug, G., Jancke, L., Huang, Y., and Steinmetz, H. 1995. In vivo evidence of structural brain asymmetry in musicians. *Science* **267:** 699–701.

Schleicher, A., and Zilles, K. 1990. A quantitative approach to cytoarchitectonics: Analysis of structural inhomogeneities in nervous tissue using an image analyser. *J. Microsc.* **157:** 367–381.

Schleicher, A., Amunts, K., Geyer, S., Morosan, P., and Zilles, K. 1999. Observer-independent method for microstructural parcellation of cerebral cortex: A quantitative approach to cytoarchitectonics. *NeuroImage* **9:** 165–177.

Schmid, N., Tschopp, K., Schillinger, C., Bilecen, D., Scheffler, K., and Seelig, J. 1998. Visualization of central auditory processes with functional magnetic resonance tomography. *Laryngorhinootologie* **77:** 328–331.

Schormann, T., von Matthey, M., Dabringhaus, A., and Zilles, K. 1993. Alignment of 3-D brain data sets originating from MR and histology. *Bioimaging* **1:** 119–128.

Schormann, T., Dabringhaus, A., and Zilles, K. 1995. Statistics of deformation in histology and application to improved alignment with MRI. *IEEE Trans. Med. Imag.* **14:** 25–35.

Schormann, T., Henn, S. and Zilles, K. 1996. A new approach to fast elastic alignment with application to human brains. *Lect. Notes Comput. Sci.* **1131:** 437–442.

Schormann, T., and Zilles, K. 1997. Limitations of the principal-axes theory. *IEEE Trans. Med. Imag.* **16:** 942–947.

Schormann, T., and Zilles, K. 1998. Three-dimensional linear and nonlinear transformations: An integration of light microscopical and MRI data. *Hum. Brain Mapp.* **6:** 339–347.

Seldon, H. L. 1981. Structure of human auditory cortex. I. Cytoarchitectonics and dendritic distributions. *Brain Res.* **229:** 277–294.

Shaywitz, B. A., Shaywitz, S. E., Pugh, K. R., Constable, R. T., Skudlarski, P., Fulbright, R. K., Bronen, R. A., Fletcher, J. M., Shankweiler, D. P., and Katz, L. 1995. Sex differences in the functional organization of the brain for language. *Nature* **373:** 607–609.

Steinmetz, H., Rademacher, J., Huang, Y. X., Hefter, H., Zilles, K., Thron, A., and Freund, H. J. 1989. Cerebral asymmetry: MR planimetry of the human planum temporale. *J. Comput. Assist. Tomogr.* **13:** 996–1005.

Steinmetz, H., Rademacher, J., Jancke, L., Huang, Y. X., Thron, A., and Zilles, K. 1990. Total surface of temporoparietal intrasylvian cortex: Diverging left–right asymmetries. *Brain Lang.* **39:** 357–372.

Strainer, J. C., Ulmer, J. L., Yetkin, F. Z., Haughton, V. M., Daniels, D. L., and Millen, S. J. 1997. Functional MR of the primary auditory cortex: An analysis of pure tone activation and tone discrimination. *Am. J. Neuroradiol.* **18:** 601–610.

Talairach, J., and Tournoux, P. 1988. *Coplanar Sterotaxic Atlas of the Human Brain.* Thieme, Stuttgart.

Talavage, T. M., Ledden, P. J., Sereno, M. I., Benson, R. R., and Rosen, B. R. 1996. Preliminary fMRI evidence for tonotopicity in human auditory cortex. *NeuroImage* **3:** 355.

Talavage, T. M., Ledden, P. J., Sereno, M. I., Rosen, B. R., and Dale, A. M. 1997. Multiple phase-encoded tonotopic maps in human auditory cortex. *NeuroImage* **5:** 8.

Talavage, T. M., Edmister, W. B., Ledden, P. J., and Weisskoff, R. M. 1999. Quantitative assessment of auditory cortex responses induced by imager acoustic noise. *Hum. Brain Mapp.* **7:** 79–88.

Thompson, P. M., Schwartz, C., Lin, R. T., Khan, A. A., and Toga, A. W. 1996. Three-dimensional statistical analysis of sulcal variability in the human brain. *J. Neurosci.* **16:** 4261–4274.

Tiitinen, H., Alho, K., Huotilainen, M., Ilmoniemi, R. J., Simola, J., and Naatanen, R. 1993. Tonotopic auditory cortex and the magnetoencephalographic (MEG) equivalent of the mismatch negativity. *Psychophysiology* **30:** 537–540.

Verkindt, C., Bertrand, O., Perrin, F., Echallier, J. F., and Pernier, J. 1995. Tonotopic organization of the human auditory cortex: N100 topography and multiple dipole model analysis. *Electroencephalogr. Clin. Neurophysiol.* **96:** 143–156.

Witelson, S. F., and Kigar, D. L. 1992. Sylvian fissure morphology and asymmetry in men and women: Bilateral differences in relation to handedness in men. *J. Comp. Neurol.* **323:** 326–340.

Witelson, S. F., Glezer, I. I., and Kigar, D. L. 1995. Women have greater density of neurons in posterior temporal cortex. *J. Neurosci.* **15:** 3418–3428.

Wree, A., Schleicher, A., and Zilles, K. 1982. Estimation of volume fractions in nervous tissue with an image analyzer. *J. Neurosci. Methods* **6:** 29–43.

Yamamoto, T., Uemura, T., and Llinas, R. 1992. Tonotopic organization of human auditory cortex revealed by multi-channel SQUID system. *Acta Otolaryngol. Stockholm* **112:** 201–204.

Yoshiura, T., Ueno, S., Iramina, K., and Masuda, K. 1995. Source localization of middle latency auditory evoked magnetic fields. *Brain Res.* **703:** 139–144.

Zilles, K. 1990. Cortex. In *The Human Nervous System* (G. Paxinos, Ed.). Academic Press, San Diego.

Zilles, K., Schlaug, G., Matelli, M., Luppino, G., Schleicher, A., Qu, M., Dabringhaus, A., Seitz, R., and Roland, P. E. 1995. Mapping of human and macaque sensorimotor areas by integrating architectonic, transmitter receptor, MRI and PET data. *J. Anat.* **187:** 515–537.

Zouridakis, G., Simos, P. G., and Papanicolaou, A. C. 1998. Multiple bilaterally asymmetric cortical sources account for the auditory N1m component. *Brain Topogr.* **10:** 183–189.